Available online www.jocpr.com

Journal of Chemical and Pharmaceutical Research, 2017, 9(5):65-72

Research Article

ISSN : 0975-7384
CODEN(USA) : JCPRC5

In Silico Molecular Docking Analysis Of Orientin, A Potent Glycoside of Luteolin against BCL-2 Family Proteins

Kalaiyarasu Thangaraj[1], Karthiga Arumugasamy[2], Karthi Natesan[1,3], Shanmugam Ramasamy[2], Ravi Cyril[2], Sanjeev Kumar Singh[4*] and Manju Vaiyapuri[1]

[1]Department of Biochemistry, Periyar University, Salem, Tamil Nadu, India
[2]Department of Zoology, Thiagarajar College, Madurai, Tamil Nadu, India
[3]Division of Biotechnology, Advanced Institute of Environment and Bioscience, Safety, Environment and Life Science Institute, College of Environmental and Bioresource Sciences, Chonbuk National University, Iksan, South Korea
[4]Computer Aided Drug Designing and Molecular Modeling Lab, Department of Bioinformatics, Alagappa University, Karaikudi, Tamil Nadu, India

---

ABSTRACT

Apoptosis is an implicit cell suicide pathway which plays a pivotal role in both normal and pathophysiological conditions. The intrinsic apoptotic pathway is tightly regulated by BCL-2 family proteins. In order to trigger apoptosis in cancerous cells, several chemotherapeutic agents were being used as anticancer agents, but still novel compounds are explored for enhanced chemoprevention. The computational approaches towards screening of active compounds made easier to ascertain their possible mechanism of action before experimental trials. Orientin, the C-glycoside of luteolin (Luteolin-8-C-glucoside) is known to exert the promising cytotoxic effect in human cancer cell lines. However, the target specific mechanism of Orientin has been not elucidated. The present study dealt with Glide XP and QPLD approach to substantiate the binding capacity of Orientin with that of apoptotic proteins which regulate the homeostasis. Further, the binding free energy calculation and pharmacokinetic properties also predicted. Overall, experimental findings suggested that Orientin has the inhibitory activity against anti-apoptotic proteins and exhibited the drug like characteristics. The insights obtained from the present work can be facilitated to carry out the experimental analysis to verify the anticancer effect of Orientin.

Keywords: Orientin; Apoptosis; BCL-2; BCL-XL; XP; QPLD

INTRODUCTION

Apoptosis is a morphologically distinct and energy dependent form of programmed cell death, much essential for the body homeostasis mechanism [1]. It is triggered by multi faceted pathways and regulated by mitochondrial mediated intrinsic and extrinsic death receptors [2]. Apoptosis is characterized by plasma membrane blebbing, cell shrinkage, chromatin condensation and chromosomal nuclear fragmentation [3] and linked to health complications such as autoimmune disorders, ischemic damage, neurodegenerative diseases, cancer and diabetes [4].

The intracellular proteins of B-cell lymphoma 2 family (BCL-2) play a major role in intrinsic apoptosis regulation and cell proliferation [5]. BCL-2 family proteins regulate both pro-apoptotic and anti-apoptotic intracellular signals and thereby mediating the mitochondrial membrane potential [6]. The dysregulation of BCL-2 family proteins leads to apoptosis evasion which eventually results in incessant cell proliferation and thereby results in cancer progression. The pro-apoptotic effectors Bax and Bak in the BCL-2 family promotes the mitochondrial permeability and elicits cytochrome C and pro-apoptotic factors into the cytosol, thereby switching on the apoptotic cascade [7]. The over expression of anti-apoptotic BCL-2 family proteins (BCL-2 and BCL-XL) commonly found in all types of human cancers such as hepatic, colorectal, breast, lung and

ovarian cancer. The functional blockade of anti-apoptotic proteins causes restoration of apoptotic mechanism in cancerous cells thereby inhibits carcinogenesis.

Targeting the apoptotic proteins, specifically the BCL-2 family proteins have become an attractive strategy for the treatment of cancer [8]. Despite the huge array of active molecules for the inhibition of apoptosis to promote anticancer efficacy, exploration of novel anticancer chemotherapeutic agents is being encouraged to pervert the cellular proliferation mechanisms. Earlier studies have established the anticancer properties of luteolin, a citrus flavonoid in colon, liver, lung cancer, head and neck cancer, prostate, breast, cervical, and skin cancer [9]. Luteolin triggers cell death via activation of apoptotic intracellular signals through cleavage of pro-apoptotic BCL-2 proteins, such as Bad and Bax and anti-apoptotic BCL-2 proteins, such as BCL-2 and BCL-XL [10].

Orientin, a potent glycoside of luteolin also expected to exhibit similar pharmacological properties. It is a water-soluble flavonoid C-glycoside with molecular formula of $C_{21}H_{20}O_{11}$ and a molecular weight of 448.3769 g/mol. It consists of mostly phenol groups with two ether groups and one ketone group. It has been isolated from various medicinal plants such as *Ocimum sanctum*, *Phyllostachys* species (Bamboo Leaves), *Passiflora* species (Passion Flowers), *Trollius* species (Golden Queen) and *Jatropha gossypifolia* (Bellyache Bush) [11]. Earlier studies have shown that Orientin (luteolin-8-glucoside) exhibited antioxidant, anti-inflammatory, neuroprotective, cardioprotective and antitumour effects [12,13]. Orientin attenuated chemically induced inflammatory bowel conditions [14] and reported cytotoxicity in EC109 cells [15] and MCF-7 cells [16].

The *in silico* docking analysis aims to identify the exact conformation of ligand in the active site of protein and determining their binding affinity. Among the different widely used docking programs, Schrodinger Glide™ was considered to be the most accurate tool for conformational studies [17]. Most of the drugs often fail in their pharmacokinetics profiling; hence, it is vital to determine the ADME property of the drug as per Lipinski's rule [18]. The present study was designed to investigate whether the Orientin could interact with the anti-apoptotic BCL2 family proteins, such as BCL-2 and BCL-XL through Glide docking analysis and prediction of ADME properties.

EXPERIMENTAL SECTION

The present study aims to explore the possible mechanism of interaction between the C-glycosyl flavanoid Orientin and anti-apoptotic proteins (BCL-2 and BCL-XL) by analyzing their binding interactions through Extra Precision (XP) and Quantumn polarized ligand docking (QPLD). For a comparative analysis, the potent anti-cancer drug, Irinotecan was used as positive drug control. The overall schematic design of the study is illustrated in Figure 1.

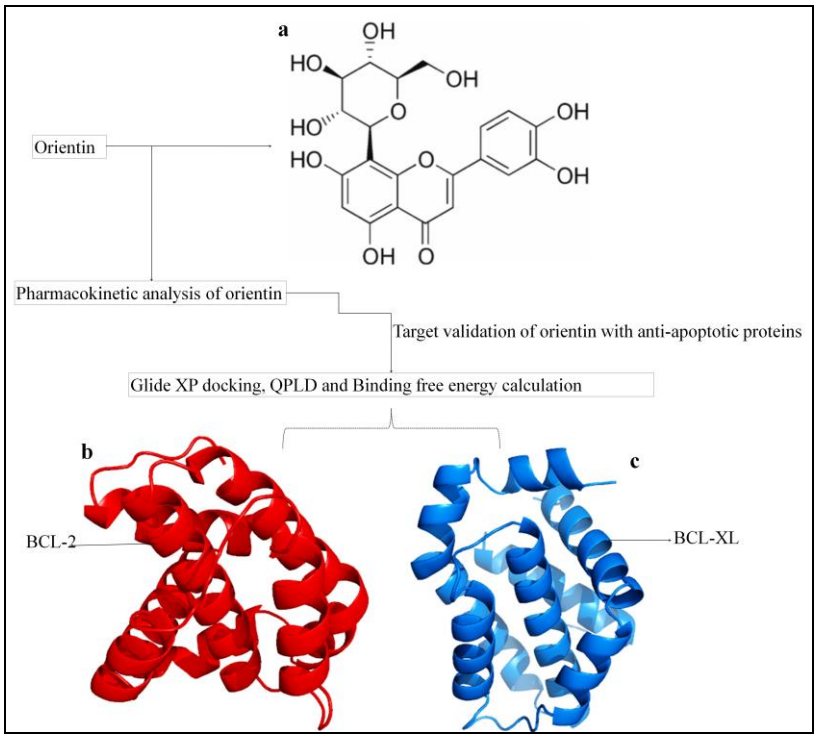

Figure 1: Schematic design of the study a) 2D-structure of Orientin b) Anti-apototic protein BCL-2 (PDB ID: 2W3L) c) Anti-apototic protein BCL-XL (PDBID: 2YXJ)

Protein identification and preparation

The crystal structure of BCL-2 (2W3L) and BCL-XL (2YXJ) were retrieved from protein data bank (PDB) for docking analysis. The Protein Prep Wizard module pre-processed the receptor protein structures for the docking analysis [19]. H-atoms are added to all the protein residues. The protonated states of His, Asp and Glu residue, hydrogens on hydroxyls and thiols were sampled to optimize the H-bond network. The standard mode performed for all the states of H-bond clusters with up to 100 combinations and Monte Carlo sampling for clusters with more than 100 possible states. The missing side chains of each residue were aligned using build interface provided by Schrodinger. The optimized protein minimization state was carried out with an impact refinement module, using OPLS-2005 force field to steric clashes that may exist in the structures. The minimization was terminated while the average root mean square value of non hydrogen atoms reached the 0.3 Å [20].

Ligand preparation

Orientin and Irinotecan ligands were prepared for structure optimization and conformer generation using LigPrep (LigPrep 3.5, 2015) [21]. The OPLS-2005 force field was applied to acquire the optimized and energy minimized conformers of ligands. Prior to the energy minimization process of ligand structures, the following steps were taken: addition of implicit hydrogen atoms, neutralization of charged groups and generation of various ionizations, tautomerization and chirality states of the ligand molecule [20].

Glide extra precision (XP) docking

The prior prepared crystal structure of proteins was taken for docking simulation. The grid box was generated at centroid of the active site for ligand interaction with defined Cartesian co-ordinates. The grid box defines the shape and properties of the active site that provide the specific binding pose to the ligand. The Coulomb and van der Waals electric field of the protein also gathered in grid box (Glide 6.9, 2015) [22]. The ligands were first docked with active site using extra precision mode (XP) an exhaustive search of possible positions and orientations over the active site of protein. To soften the van der Waals radii of nonpolar receptor atoms, the scaling factor set as 1.0 and partial atomic charge cutoff as 0.25. The grid box size was defined with 10 Å radii around the ligand from active site. OPLS-2005 force field was employed for refinement of docking solutions including the torsional and rigid body movements of the ligand used. In XP docking, the GlideScore is more accurate at minimizing false positives, especially in lead optimization. The small numbers of lowest energy poses are taken for Monte Carlo simulation (Glide 6.9, 2015) [22]. Finally, the binding affinity of receptor-ligand was ranked by GlideScore and poses in ligand databases. The docked models were graded using Emodel energy, composite scoring of receptor-ligand molecular mechanics interaction and ligand strain energy [19].

Quantum polarized ligand docking

The Quantum-Polarized Ligand Docking (QPLD) enhance the partial charges on the ligand atoms in a Glide docking run by replacing them with charges derived from quantum mechanical calculations. In QPLD, selected ligands were docked with Glide, then charges induced by the protein on the ligand are calculated and a set of the best ligand poses are redocked (QM-Polarized Ligand docking protocol, 2015) [23]. QPLD merged the potential of Quantum mechanics and Molecular mechanics (QM/MM) (accuracy/speed). The combined QM/MM approach enhances the accuracy and minimizes the period to calculate the atomistic level prediction of charge transition and binding energy. QPLD employed QM calculation only for ligand and binding site of protein and the rest of the protein regions processed by MM force field calculation [24,25]. To alleviate the potential for non-polar part of the receptor, van der Waal radii of receptor atoms were scaled by 2.00 Å with a partial charge cut-off 0.25. The selection of QM level for charge calculation is an exchange between speed and accuracy. The partial charges of the ligand calculated from surface electrostatic potential energy by fast and accurate modes. Fast employs the 3-21G basis set, B3LYP functional and 'Quick' self-consistent field (SCF) accuracy level. Next, accurate employs the 6-31G⁄LACVP⁄ basis set, B3LYP and 'Ultrafine' SCF accuracy level (iacc=1, iacscf=2) for the functional theory calculation in the QM region. The ligand and active site region were treated quantum mechanically and the rest of the protein system was treated as molecular mechanics mode.

Binding free energy calculation

The docked complex was subjected to the binding free energy calculation using Molecular Mechanics Generalized Born Surface Area (MM-GBSA) approach employed by Prime 3.0 (Prime 3.0, 2015.) [26]. The scoring functions may fail if they do not properly account for solvation, entropy or polarizability. OPLS-2005 force field and GBSA continuum solvent model were used to validate the accuracy of the docking score which confirmed the stability of the docking complex. Binding energy was calculated by the following equations [24],

$$\Delta G_{bind} = \Delta E + \Delta G_{solv} + \Delta G_{SA} \quad (1)$$

$$\Delta E = E_{complex} - E_{protein} - E_{ligand} \quad (2)$$

where, ($E_{complex}$, $E_{protein}$, and E_{ligand} are the minimized energies of the protein-inhibitor complex, protein, and inhibitor, respectively).

$$\Delta G_{solv} = G_{solv}(complex) - G_{solv}(protein) - G_{solv}(ligand) \quad (3)$$

where, ΔG_{solv} is generalized born electrostatic solvation energy. G_{solv}(complex), G_{solv}(protein) and G_{solv}(ligand) are the solvation free energies of complex, protein and ligand respectively.

$$\Delta G_{SA} = G_{SA}(complex) - G_{SA}(protein) - G_{SA}(ligand) \quad (4)$$

where, ΔG_{SA} is the non-polar contribution to the solvation energy due to the surface area. G_{SA}(complex), G_{SA}(protein) and G_{SA}(ligand) are the surface energies of complex, protein and ligand respectively.

The simulations were carried out using the GBSA continuum model. Prime uses a surface generalized Born (SGB) model employing a Gaussian surface instead of a van der Waals surface for better representation of the solvent-accessible surface area (Prime 3.0, 2015) [26].

ADME prediction

ADME properties were calculated for the phase searched chemical databases using QikProp which predicts the physicochemical properties and pharmacologically relevant properties of the lead molecule (QikProp 4.4, 2015) [27]. All the known and unknown molecules were neutralized before the QikProp analysis. QikProp follows the BOSS program with OPLS-AA force field to perform Monte Carlo statistical mechanics simulations on organic solutes in a periodic box of explicit water molecules. This simulation leads to configurationally average for number of pharmacological descriptors; correlations of these descriptors to experimentally determined properties were compared (QikProp 4.4, 2015) [27]. The program was performed with normal mode to investigate the pharmacological properties of the known and screened compounds.

RESULTS AND DISCUSSION

Apoptotic cell death is widely considered as an optimistic process that both prevents and treats cancer [28]. BCL-2 family proteins play a major regulatory role in apoptosis. If a compound or ligand interacts with the catalytic site of the targeted protein, it will diminish the activity of protein and alter the protein conformation. The interaction between the ligand and protein relies upon the hydrogen bonding. The quantity of hydrogen bond interaction determines the inhibitory ability of the compound towards protein [29].

In our study, the possible binding patterns and interaction mechanisms of Orientin were analyzed using Glide docking tool and evaluated using GlideScore and binding energies. In general, Glide score represents the best fit for a ligand in the active site of the target macromolecule [30]. They were evaluated based on the interaction of Orientin in the active site of BCL-2 and BCL-XL proteins.

Glide XP docking and QPLD analysis

A comparative analysis between Glide XP docking and QPLD scoring and pose interaction confirmed the significant binding affinity of Orientin. The interaction map of Orientin and Irinotecan were illustrated in Figures 2 to 5 (Tables 1-4).

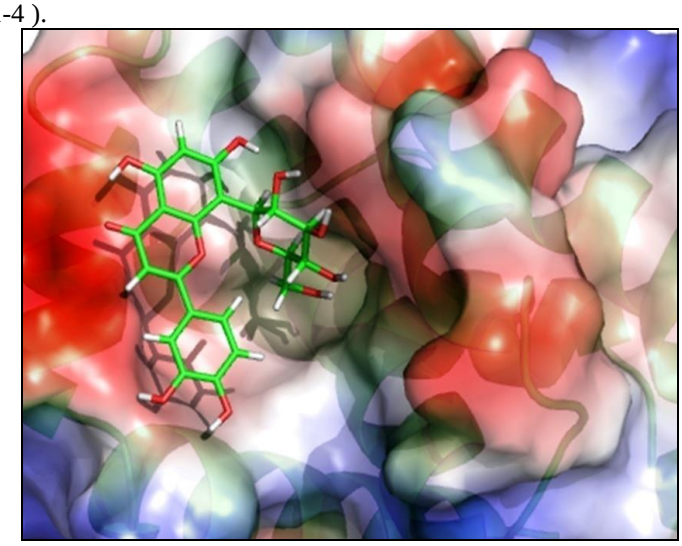

Figure 2: Electrostatic potential at the surface of the active site of BCL-2 bound with Orientin (the green stick model). The negative, positive and neutral charge of the binding site residues were denoted as red, blue and white color respectively

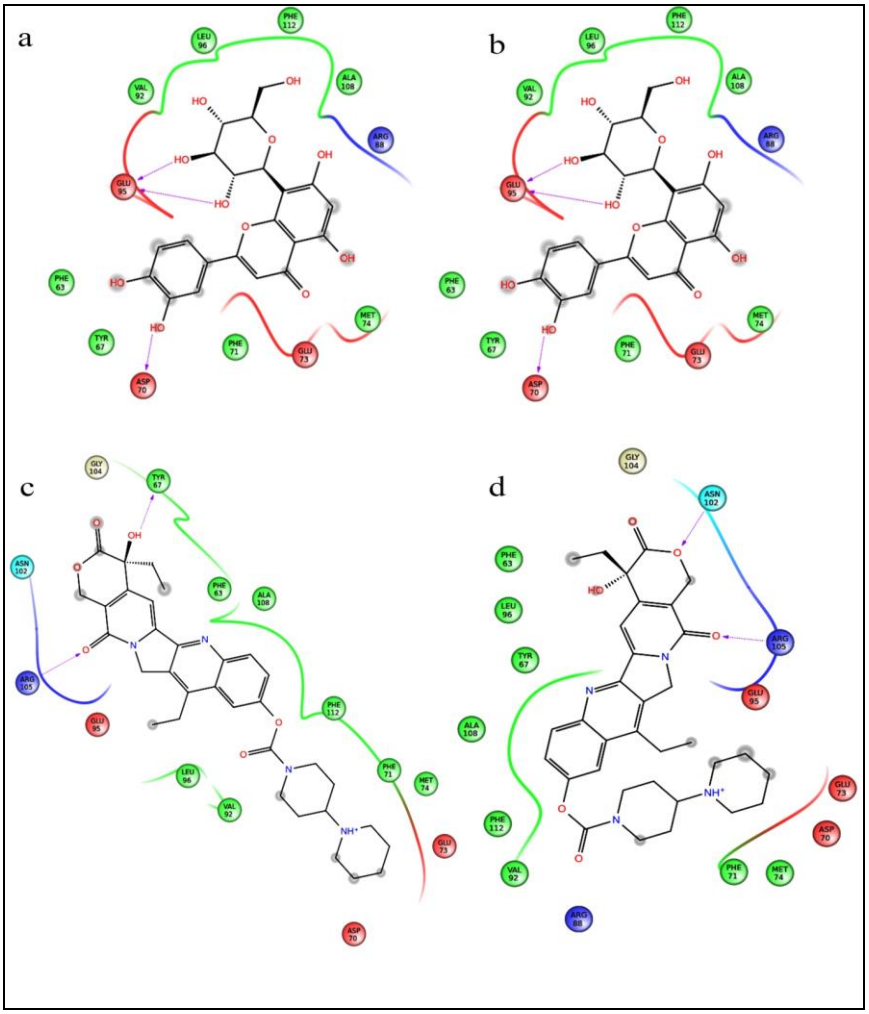

Figure 3: Docking poses of BCL-2 - drug complexes. (a) XP docking map of Orientin-BCL-2 complex (b) QPLD map of Orientin-BCL-2 complex (c) XP docking map of Irinotecan-BCL-2 complex (d) QPLD map of Irinotecan-BCL-2 complex

Table 1: Glide XP docking scores and docking poses of BCL-2 – Orientin complex

Compound	Docking score*	Glide energy	Glide Emodel energy	H-bonds	Non-H-bond interaction	Interacting residue
Orientin	-6.77	-40.85	-50.68	3	-	Glu95,Asp70
Irinotecan	-4.57	-47.33	-67.72	2	-	Arg105, Tyr67

Table 2: QPLD scores and docking poses of BCL-2 – Orientin complex

Compound	Docking score*	Glide energy	Glide Emodel energy	H-bonds	Non-H-bond interaction	Interacting residue
Orientin	-4.26	-38.44	-46.42	2	1	Glu95, Asp70, Arg88
Irinotecan	-5.8	-46.93	-62.96	2	-	Asn102,Arg105

Table 3: Glide XP docking scores and docking poses of BCL-XL – Orientin complex

Compound	Docking score*	Glide energy	Glide Emodel energy	H-bonds	Non-H-bond interaction	Interacting residue
Orientin	-7.69	-40.38	-62.84	3	1	Leu130,Glu129,Arg139
Irinotecan	-6.91	-5.95	-68.89	1	-	Asn136

Table 4: QPLD scores of and docking poses BCL-XL – Orientin complex

Compound	Docking score*	Glide energy	Glide Emodel energy	H-bonds	Non-H-bond interaction	Interacting residue
Orientin	-4.01	-35.28	-43.14	4	-	Glu129, Leu130, Asp133
Irinotecan	-5.8	-46.93	-62.96	1	-	Asn136

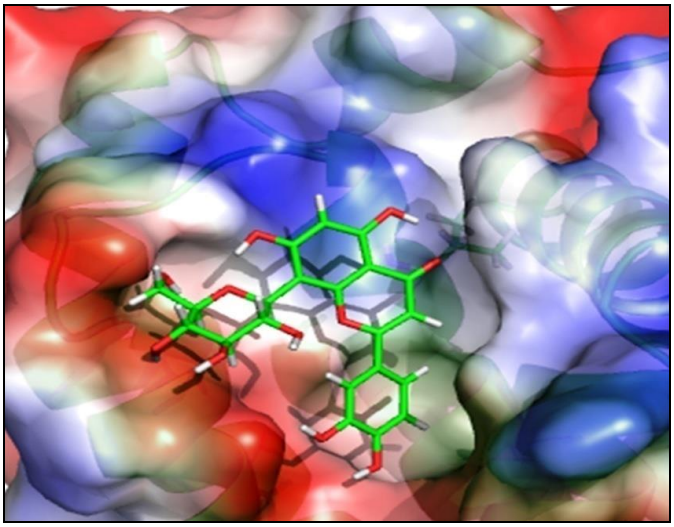

Figure 4: Electrostatic potential at the surface of the active site of BCL-XL bound with Orientin (the green stick model). The negative, positive and neutral charge of the binding site residues were denoted as red, blue and white color respectively

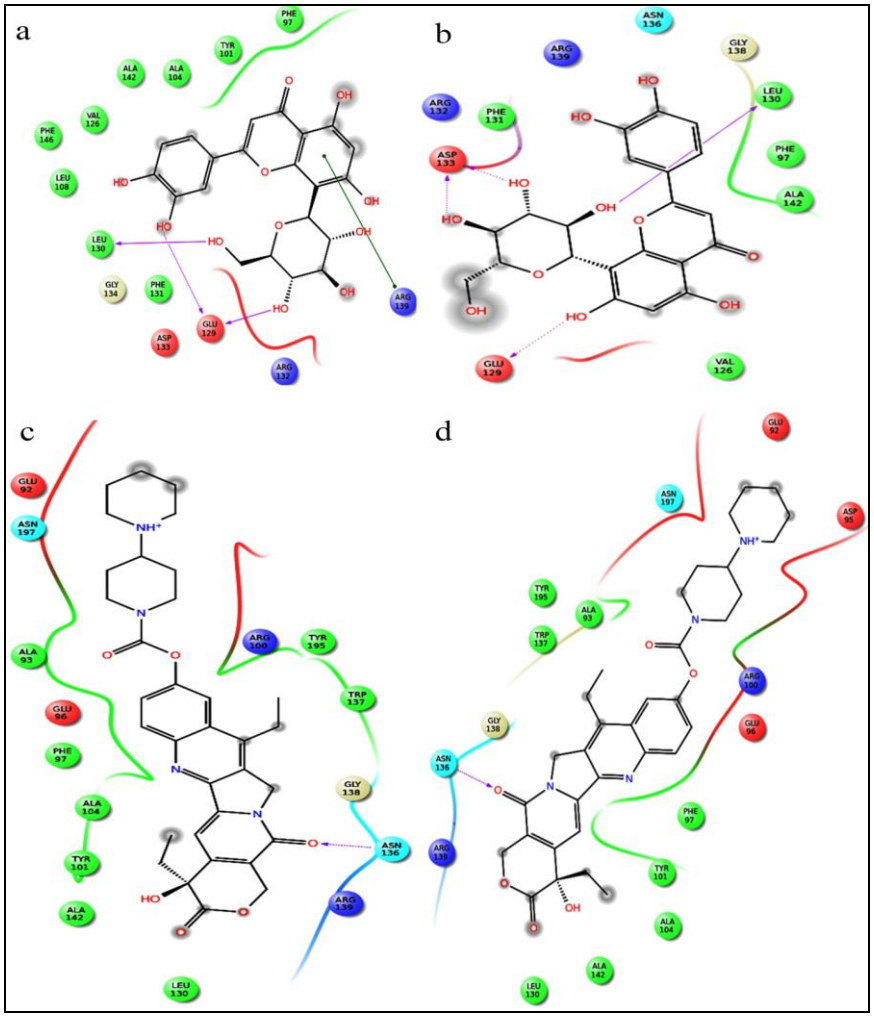

Figure 5: Docking poses of BCL-XL - drug complexes. (a) XP docking map of Orientin-BCL-2 complex (b) QPLD map of Orientin-BCL-2 complex (c) XP docking map of Irinotecan-BCL-2 complex (d) QPLD map of Irinotecan-BCL-2 complex

Glide XP and QPLD docking score, Emodel energy score of Orientin against target receptors were described in Tables 1 to 5. The electrostatic potential surface of binding pocket of BCL-2 with Orientin has illustrated in Figure 2. In BCL-2, Orientin exhibited three hydrogen bond with Glu95 and Asp70 active site residues whilst the Glide XP docking. In QPLD, two hydrogen bond interactions formed with Glu95 and Asp70 residues of BCL-2; one π-π stacking with Arg88 (Figures 3a and 3b). The predicted docking score of Glide XP docking and

QPLD were -6.77 and -4.26 kcal/mol respectively. Irinotecan formed two hydrogen bonds with Arg105, and Tyr67 in Glide XP docking mode and interact with Asn102 and Arg105 residues in QPLD analysis (Figures 3c and 3d). The docking score of Glide XP docking and QPLD were -4.57 and -5.80 kcal/mol respectively.

Binding free energy calculation

The docking complex was evaluated using a related post-scoring approach, MM-GBSA. The results from the binding free energy prediction using MM-GBSA are listed in the Table 5. It is found that the binding free energies of BCL-2 and BCL-XL Orientin complex were -39.61 and -40.32 kcal/mol respectively.

Table 5: Binding free energy Binding free energy calculation of protein-Orientin complex using MM/GBSA method

Protein	Orientin				Irinotecan			
	$\Delta G_{couloumb}$ [a]	ΔG_{vdw} [b]	$\Delta G_{solLipo}$ [c]	ΔG_{bind} [d]	$\Delta G_{couloumb}$ [a]	ΔG_{vdw} [b]	$\Delta G_{solLipo}$ [c]	ΔG_{bind} [d]
BCL-2	-24.48	-30.85	-14.91	-39.61	-32.98	-44.11	-22.42	-43.96
BCL-XL	-34.39	-27.7	-12.26	-40.32	-51.63	-52.18	-21.79	-62.59

*All the energy values in kilocalories per mole (Kcal/mol); [a]Contribution to the free energy of binding from the Coulomb energy; [b]Contribution to the free energy of binding from the van der Waals energy; [c]Contribution to the free energy of binding from the lipohilic energy; [d]Free energy of binding

In terms of binding free energy, the major energy contributors were identified as van der Waals (ΔG_{vdw}), Colulomb interaction ($\Delta G_{Colulomb}$) and lipohilic energy ($\Delta G_{solLipo}$) that enhance the binding affinity of Orientin towards binding pocket of proteins (Table 5). Addition to the hydrogen bond interaction the non-bonded interaction also plays equipotent role in protein-ligand complex stability.

QikProp analysis

The Orientin and Irinotecan was further evaluated for pharmacokinetic property analysis to predict the physicochemical and biological features. The descriptors of volume, hydrogen bond donor and acceptors, polarizability, total solvent accessible surface area, and rule of five parameters were chosen for the prediction.

Table 6 : ADME property of Orientin

Descriptors*	Orientin	Irinotecan	Accepted range
donorHB	7	1	0.0 – 6.0
accptHB	13	12.75	2.0 – 20.0
QPpolrz	38.84	63.62	13.0 – 70.0
SASA	672.89	939.55	300.0 – 1000.0
PISA	189.31	141.55	0.0 – 450.0
Volume	1223.54	1774.07	500.0– 2000.0
Rule of Five	2	1	Maximum is 4

donorHB- Estimated number of hydrogen bonds that would be donated by the solute to water molecules in an aqueous solution. Values are averages taken over a number of configurations, so they can be non-integer.; **accptHB** - Estimated number of hydrogen bonds that would be accepted by the solute from water molecules in an aqueous solution. Values are averages taken over a number of configurations, so they can be non-integer; **QPpolrz** - Predicted polarizability in cubic angstroms; **SASA** Total solvent accessible surface area (SASA) in square angstroms; using a probe with a 1.4 Å radius; **PISA**-π (carbon and attached hydrogen) component of the SASA; **Volume** - Total solvent-accessible volume in cubic angstroms using a probe with a 1.4 Å radius; **Rule of Five-** Number of violations of Lipinski's rule of five. The rules are: mol_MW < 500, QPlogPo/w < 5, donorHB ≤ 5, acceptHB ≤ 10. Compounds that satisfy these rules are considered druglike. (The "five" refers to the limits, which are multiples of 5)

Volume parameter is explained as total solvent-accessible volume in cubic angstroms and exhibited range from 1223.54 - 1774.07. Estimated number of hydrogen bond donor and acceptor range from 1-7and 12.75-13 respectively. The SASA is ranged from 672.89 to 939.55 and PISA range from 141.55 to 189.31, all the predicted values were accomplishing the desired range (Table 6). The predicted value of rule of five is 1 to 2. The polarizability also exhibited the significant range value of 38.84 to 63.62.

CONCLUSION

The present study explores the binding specificity of Orientin against anti-apoptotic proteins of BCL-2 and BCL-XL. The specific interaction of Orientin was analyzed by different docking techniques such as Glide XP docking and QPLD. The binding stability and interaction of Orientin was further evaluated by MM/GBSA based binding free energy calculation. The binding mode of Orientin is compared and verified with known Irinotecan drug. According to the finding, Orientin followed the similar binding pattern of Irinotecan as well as showed additional interaction with active sites of BCL-2 and BCL-XL. The pharmacokinetic property prediction also supported the drug likeness of Orientin. Thus, Orientin would be subjected to further experimental analysis in order to confirm the antitumor effect.

ACKNOWLEDGEMENTS

The first author acknowledges the financial assistance under University Research Fellowship, Periyar University, Salem, Tamil Nadu, India.

Declaration of Conflicting Interests

The author(s) declared no potential conflicts of interest with respect to the research, authorship, and/or publication of this article.

REFERENCES

[1] H Dai; XW Meng; SH Kaufmann. *Cancer Transl Med*. **2016**, 2(1), 7.
[2] P Antony; R Vijayan, R. *Drug Des Devel Ther*. **2016**, 10, 1399.
[3] A Dasgupta; M Nomura; R Shuck; J Yustein. *Intl J Mol Sci*. **2016,** 18(1), 23.
[4] G Pistritto; D Trisciuoglio; C Ceci; A Garufi; G D'Orazi. *Aging (Albany NY)*. **2016**, 8(4), 603.
[5] H Akl; T Vervloessem; S Kiviluoto; M Bittremieux; JB Parys; H De Smedt; G Bultynck. *Biochim Biophys Acta*. **2014**, 1843(10), 2240-2252.
[6] A Ashkenazi; WJ Fairbrother; JD Leverson; AJ Souers. *Nat Rev Drug Discov*. **2017**.
[7] T Vervliet; JB Parys; G Bultynck. *Oncogene*. **2016**, 35(39), 5079-5092.
[8] JL Fox; M MacFarlane. *Br J Cancer*. **2016**.
[9] M Vaiyapuri; N Namasivayam. *J Biochem Technol.* **2009**, 1(2), 57-61.
[10] D Majumdar; KH Jung, H X Zhang; S Nannapaneni; X Wang; AR Amin; Z Chen; DM Shin. *Cancer Prev Res*. **2014,** 7(1), 65-73.
[11] KY Lam; APK Ling; RY Koh; YP Wong; YH Say. *Adv Pharmacol Sci*. **2016**.
[12] SK Ku; S Kwak; JS Bae. *Inflammation.* **2014**, 37(6), 2164-2173.
[13] BNT Law; APK Ling; RY Koh, SM Chye; YP Wong. *Mol Med Rep*. **2014**, 9(3), 947-954.
[14] A Sun; G Ren; C Deng; J Zhang; X Luo; X Wu; S Mani; W Dou; Z Wang. *J Funct Foods.* **2016**, 21, 418-430.
[15] F An; S Wang; Q Tian; D Zhu. *Oncol Lett*. **2015**. 10(4), 2627-2633.
[16] M Czemplik; J Mierziak; J Szopa; A Kulma. *Front Pharmacol*. **2016**, 7.
[17] SK Tripathi; R Muttineni; SK Singh. *J Theor Boil*. **2013**, 334, 87-100.
[18] K Loganathan; K Sithick Ali. 2016. *J Chem Pharm Res*. **2016**, 8(1), 542-548.
[19] RA Friesner; JLBanks; RB Murphy; TA Halgren; JJ Klicic; DT Mainz; MP Repasky, EH Knoll; M Shelley; JK Perry; DE Shaw. *J Med Chem.* **2004**, 47(7), 1739-1749.
[20] GM Sastry; M Adzhigirey; T Day; R Annabhimoju; W Sherman. *J Comput Aided Mol Des.* **2013**, 27(3), 221-234.
[21] LigPrep version 3.3, *Schrodinger, LLC, New York, NY*, **2015**.
[22] Glide, version 6.6, *Schrodinger, LLC, New York, NY*, **2015**.
[23] AE Cho; V Guallar; BJ Berne; R Friesner. *J Comput Chem.* **2005**, 26(9), 915-931.
[24] C Selvaraj; SK Singh. *J Biomol Struct Dyn*. **2014**, 32(8), 1333-1349.
[25] QPLD, version 6.6, *Schrodinger, LLC, New York, NY*, **2015**.
[26] Prime, version 3.9, *Schrodinger, LLC, New York, NY*, **2015**.
[27] QikProp, version 4.3, *Schrodinger, LLC, New York, NY*, **2015**.
[28] G Ichim; SW Tait. A fate worse than death: apoptosis as an oncogenic process. *Nat Rev Cancer*. **2016.**
[29] A Arsianti; H Tanimoto, T Morimoto; K Kakiuchi. *Open J Med Chem.* **2014**, 4(03), 79.
[30] V Sharma; PC Sharma; V Kumar. *Adv Chem.* **2016**.